2017 International Conference on Transportation Infrastructure and Materials (ICTIM 2017)
ISBN: 978-1-60595-442-4

Micromechanics-based Analysis of Effect of Internal Structure on Creep Anisotropy of Asphalt Concrete

Deyu Zhang[1], Lijin He[2], Youxin Wei[1], and Ling Cong[1]

[1]*School of Civil Engineering and Architecture, Nanjing Institute of Technology, Nanjing 211167, China*
[2]*Guangxi Polytechnic of Construction, Nanning 530007, China*

ABSTRACT: In order to investigate the effect of internal structure on creep anisotropy of asphalt concrete (AC), a three-dimensional (3D) micromechanical model was developed using discrete element method. The digital AC specimen composed of coarse aggregates, asphalt mastic and air voids was generated. The corresponding micromechanical models among the interactions of microscale components of digital AC specimen were assigned. The microscale viscoelastic parameters were obtained from laboratory dynamic shear test. Simulation of uniaxial creep tests were conducted on a number of cubic digital AC specimens with different aggregate orientations and sphericity. It was observed that the longer projected length of aggregates in loading direction, the smaller the creep strain is. The creep strain of AC was much smaller in the major axis direction of aggregate orientation as compared with the minor one. The creep anisotropy of AC became obvious with decreasing aggregate sphericity, especially when projected length of aggregates varied greatly in different directions.

INTRODUCTION

With the increasing traffic and heavy vehicles, rutting has become one of the major distresses in asphalt pavements, and seriously affects driving safety and comfort. Since the creep behavior of asphalt concrete is closely related to rutting, it has been widely studied. Previous studies on the creep behavior of AC were based on the assumption that AC is an isotropic material. However, some recent research studies show that the bound and unbound granular materials, such as asphalt concrete[1-3], unbound aggregate bases[4,5] are anisotropic materials with pronounced direction dependent whose mechanical behaviors are very different from that of the isotropic materials.

Previous studies showed that the internal structure is closed related to anisotropy of AC, such as aggregate orientation, angularity and contact normal. Masad et al. investigated the stiffness anisotropy of AC using image processing techniques by quantifying the internal structure anisotropy in terms of the preferred orientation of longest axes and contact normals of aggregates. The orientations of the longest axes are found to be easier to measure, and better descriptors of anisotropy, than the contact normals. The stiffness in horizontal direction is shown to be up to 30% higher than the stiffness in vertical direction[1]. Liang et al. conducted confined triaxial compression test to obtain mechanical properties of various HMA specimens with three orientation angles (0, 45, and 90 degrees) between the compaction direction and the axial load

direction. Results show that the behavior of the AC mixtures was found to be direction dependent and the anisotropic behavior of the AC mixtures could be related to the aggregate orientation. The researcher also suggested carrying out investigations to evaluate the effect of the aggregate particles distribution, orientation, shape, and angularity on the anisotropic response of the AC[6]. Zhang et al. modified the original formulation of the vector magnitude to account for the size, orientation, and sphericity of coarse and fine aggregates. Nondestructive tests were conducted to quantify the influence of the inherent microstructure of the aggregates on the anisotropy of the mixtures. The modulus ratio of the vertical modulus to the horizontal modulus is found to depend solely on the aggregate characteristics including the inclination angle, size, and sphericity [7].

By summarizing research studies above, the AC specimens in these studies were all laboratory-compacted. However, the internal structure of the AC specimens can not be accurately controlled due to the variability of laboratory-compacted specimens. This may lead to inaccurate relationship between the anisotropy of AC and its internal structure. Therefore, this paper developed a 3D DE model of AC to investigate the effect of its internal structure on creep anisotropy. The digital AC specimen is composed of coarse aggregates, asphalt mastic and air voids, in which the internal structure could be desirably controlled. The uniaxial creep tests were performed on the digital AC specimens in horizontal and vertical directions and the effect of aggregate orientation and sphericity on creep anisotropy of AC were investigated.

PREPARATION OF 3D DISCRETE ELEMENT MODEL

3D DIGITAL SPECIMEN OF AC

Asphalt concrete is composed of aggregates, asphalt binder and air voids. In order to take account of computing efficiency and obtaining viscoelastic parameters of asphalt mastic, the aggregates larger than 1.18 mm were regarded as coarse aggregates. The aggregates smaller than1.18 mm and asphalt binder were regarded as homogeneous asphalt mastic. Therefore, the digital AC specimen developed in this paper was composed of coarse aggregates, asphalt mastic and air voids.

According to the target asphalt content, air void level and aggregate gradation (as shown in Table 1), the aggregate volumetric fraction was calculated. Then the aggregate spheres were placed into a cylinder with the radius of 50 mm and the height of 150mm enclosed by three walls, and the “loop” command in “Fish” language embedded within PFC3D was performed to avoid overlap among the aggregates. The graded aggregate spheres were generated as shown in FIG. 1(a).

Table 1. Aggregate gradation.

Sieve size /mm	19	16	13.2	9.5	4.75	2.36	1.18
Percentage passing /%	100	95	84	70	48	34	24.5

After the graded aggregates were generated, 148200 face-centered packing spheres (each with six neighbors) with the radius of 1 mm were generated to fill out the cylinder, as shown in FIG. 1(b).

The previous studies showed that the aggregate morphology significantly affects the mechanical behavior of AC[8,9]. Therefore, in order to generate the aggregates with irregular shape, a generation procedure of irregular polyhedron aggregates developed by Liu was adopted in this paper. A polyhedron is formed by truncating the graded spheres with the reference planes. Then a polyhedron aggregate is generated by covering the face-centered packing spheres with the polyhedron[10]. Some of the randomly created polyhedron aggregates are shown in FIG. 2 as examples. Then the face-centered packing spheres were traversed to determine their locations. Spheres located in the polyhedron belong to the polyhedron aggregates and the remaining portion was considered as asphalt mastic and air voids. In order to increase computing efficiency, each aggregate was treated as a clump. After traversing the face-centered packing spheres, the original graded aggregate spheres were removed. After the AC specimen was initially modeled, the aggregate gradation and volumetric fraction were calculated and compared with the desired values. If the desired result is not obtained, the steps above should be repeated until the gradation and volumetric properties reach the target. The developed 3D digital AC specimen is shown in FIG. 1(c).

Since the air voids could significantly affect the creep behavior of AC, 5928 asphalt mastic discrete elements were removed randomly to form the air voids at the level of 4%. It should be noted that due to the complexity of air void distribution in the field and laboratory specimens [11, 12], the air void distribution and size were assumed to be uniform. The air void distribution in the 3D digital specimen was shown in FIG. 1(d).

(a) Graded aggregates **(b) Face-centered packing spheres** **(c) 3D digital specimen** **(d) Distribution of air voids**

Figure 1. 3D modeling illustration of asphalt mixture.

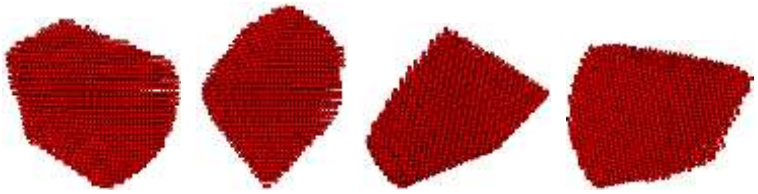

Figure 2. Randomly created polyhedron aggregates.

MICROMECHANICAL CONTACT MODEL AND PARAMETERS

Table 2. Viscoelastic parameters of asphalt mastic at 60℃.

E_1 (MPa)	η_1 (MPa·s)	E_2 (MPa)	η_2 (MPa·s)
4.64	83.34	0.82	10.00

In the DE model of asphalt concrete, there are four types of contacts to represent four different interactions: contacts within asphalt mastic, between mastic and aggregates, between adjacent aggregates, and within aggregates.

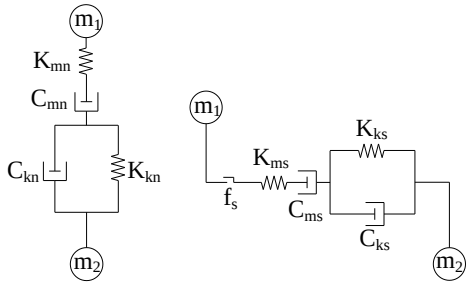

(a) Micro behaviors on normal dirction (b)Micro behaviors on shear dirction

Figure 3. Microscale Burger's model.

Considering the viscoelastic behavior of asphalt mastic, Burger's model (as shown in FIG. 3) and contact-bond model, was employed to represent the interaction within asphalt mastic and between asphalt mastic and aggregates The parameters in Burger's macroscale model used in this paper were fitted from the dynamic shear test as listed in Table 2. The conversion between Burger's microscale model parameters (as shown in FIG. 3) and macroscale material properties were developed by Liu[13].

$$K_{mn} = E_1 L \qquad C_{mn} = \eta_1 L \qquad K_{kn} = E_2 L \qquad C_{kn} = \eta_2 L \tag{1}$$

$$K_{ms} = E_1 L / 2(1+\upsilon) \qquad C_{ms} = \eta_1 L / 2(1+\upsilon)$$

$$K_{ks} = E_2 L / 2(1+\upsilon) \qquad C_{ks} = \eta_2 L / 2(1+\upsilon) \tag{2}$$

Where E_1、η_1、E_2、η_2 is Burger's macroscale model parameters, K_{mn}、C_{mn}、K_{kn}、C_{kn} is Burger's microscale model parameters on normal direction, K_{ms}、C_{ms}、K_{ks}、C_{ks} is Burger's microscale model parameters on shear direction, L is the sum of two neighboring spheres' radius, υ is Poisson ratio.

Aggregates are considered as a pure elastic material. The Linear contact-stiffness model and contact-bond model were employed to represent the interaction within aggregates. The Linear contact-stiffness model was employed to represent the interaction between adjacent aggregates. Considering the

face-centered packing spheres in the developed DE model of asphalt concrete, the micro-stiffness of aggregate elements was determined based on the following equations [14]:

$$k_n = 4ER \tag{3}$$

$$k_s = k_n / 2(1+\upsilon) \tag{4}$$

Where E is the apparent Young's modulus, k_n is the input normal stiffness, k_s is the input shear stiffness, R is the radius of the spheres.

The aggregate modulus was fixed at 55.5GPa in this study[15,16]. Since the main purpose is to investigate the creep properties of asphalt mixtures, bond breakage within the DE model was suppressed by using very high bond strength value.

SIMULATION OF UNIAXIAL CREEP TEST

On the basis of the digital AC specimen modeled above, a static load of 0.7MPa was applied on the digital specimen. As loading in PFC3D is usually performed by walls, two walls were placed onto the upper and lower specimen surfaces. Since the forces on a wall may not be specified directly, but they may be controlled by constructing a servo-mechanism in "Fish" that alters the applied velocity so as to keep the axial stress in AC specimen at a prescribed value.

Rutting usually occurs at high temperature, especially when the temperature is close to the softening point[17]. Therefore, the test temperature was set to the representative temperature of 60 ℃. The AC specimens were compacted to a cylinder with the radius of 50 mm and the height of 150mm. The optimum asphalt content is 4.6%, and the air void level is 4%. The aggregate gradation was shown in Table 1. Simulation of uniaxial creep test and laboratory experiment were conducted under the same conditions. The comparing results were shown in FIG. 4.

It can be seen from FIG. 4 that the prediction of the 3D model is very closed to the laboratory measurement, but not exactly the same. The reason may be that the aggregate morphology in the digital specimen is not exactly the same with that the real aggregate morphology, the void distribution in the digital specimen is also different from the real void distribution, and the boundary conditions of laboratory experiment are not as strict as that of the DE model. In general, the 3D DE model could give more accurate predictions to the creep behavior of AC. It is an effective tool to investigate the creep anisotropy of AC.

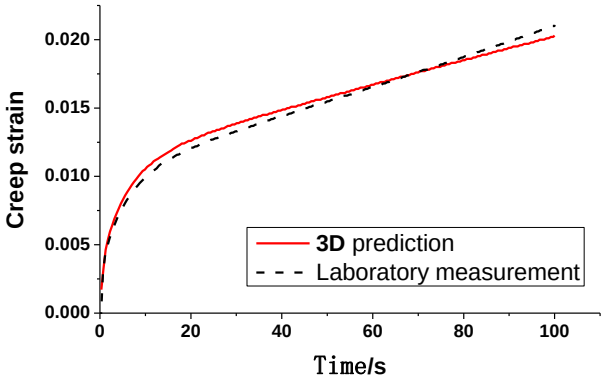

Figure 4. Comparing of results of 3D prediction and laboratory measurement.

EFFECT OF INTERNAL STRUCTURE ON CREEP ANISOTROPY OF AC

EFFECT OF AGGREGATE ORIENTATION

In order to investigate the effect of aggregate orientation on creep anisotropy, of AC, cubic digital AC specimens with the length of 10 cm were developed on the basis of the above modeling method, in which ellipsoids with different orientations represent aggregate particles. The ellipsoids are formed by a clump of discrete elements. The three principal axes of an ellipsoid represent the longest, intermediate, and shortest dimensions of the corresponding aggregate particle. The definitions of an ellipsoid and the orientation angles are given as follows.

If an ellipsoid's three principal axes are aligned on the three axes of a xyz-Cartesian coordinate system, the equation of the ellipsoid body is

$$\frac{(x-x_0)^2}{a^2}+\frac{(y-y_0)^2}{b^2}+\frac{(z-z_0)^2}{c^2}\le 1 \tag{5}$$

Where a and b are equatorial radii and c is polar radius. All variables are fixed positive real numbers determining the ellipsoid shape. (x_0, y_0, z_0) is the coordinate of the ellipsoid center. If a ≥ b ≥ c, 2a, 2b, and 2c are the longest, intermediate, and shortest dimensions of an aggregate particle, respectively. The particle size (2a) can be randomly created by using the sieve size for the given gradation shown in Table 1. In this paper, b and c were assumed to be equal.

According to the NCHRP Report 555 [18], the sphericity index (SP) is formulated as

$$SP=\sqrt[3]{\frac{b\times c}{a^2}} \tag{6}$$

In this section, the sphericity index was set to be 0.7. After the aggregate shape was determined, the ellipsoid aggregates were rotated around the y-axis, which results in the orientation angles, α. The equation of the rotated ellipsoid body is

$$\frac{x'^2}{a^2}+\frac{y'^2}{b^2}+\frac{z'^2}{c^2}\le 1 \tag{7}$$

$$\begin{cases} x'=(x-x_0)\cos\alpha+(z-z_0)\sin\alpha \\ y'=y \\ z'=(z-z_0)\cos\alpha-(x-x_0)\sin\alpha \end{cases} \tag{8}$$

Three digital AC specimens with aggregate orientations of 0°, 30°and 45° were developed, and the ellipsoid aggregates with different orientations were shown in FIG.5. Simulation of uniaxial creep tests were performed on the three cubic digital AC specimens in horizontal and vertical directions, as shown in FIG. 6. A static load of 0.7MPa was applied. The creep strain of the digital AC specimens with different aggregate orientations was shown in FIG. 7.

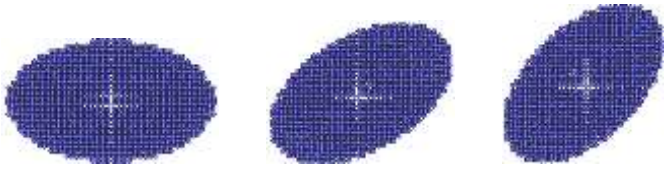

(a) α=0° (b) α=30° (c) α=45°

Figure 5. Ellipsoid aggregates with different orientations.

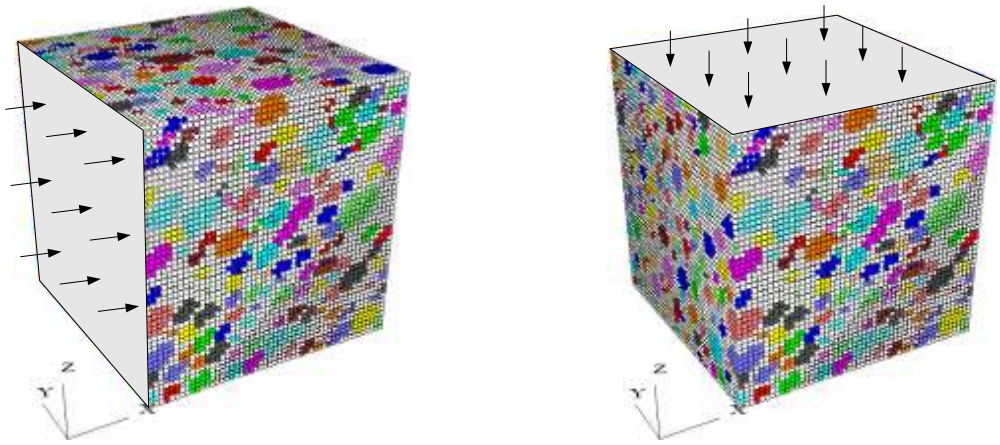

(a) Horizontal direction **(b) Vertical direction**

Figure 6. Unaxial creep test in horizontal and vertical directions.

As can be seen from FIG.7, when the aggregate orientation is 0°, the creep strain in horizontal direction is much smaller than that in vertical direction. When the aggregate orientation is varied to be 30°, the creep strain in the horizontal direction is still smaller than that in the vertical direction, but with less difference. When the aggregate orientation is varied to be 45°, there is not obvious difference between the creep strain in both directions. It was found that the longer projected length of aggregates in loading direction, the smaller the creep strain is. The creep strain of AC was much smaller in the major axis direction of aggregate orientation as compared with the minor one.

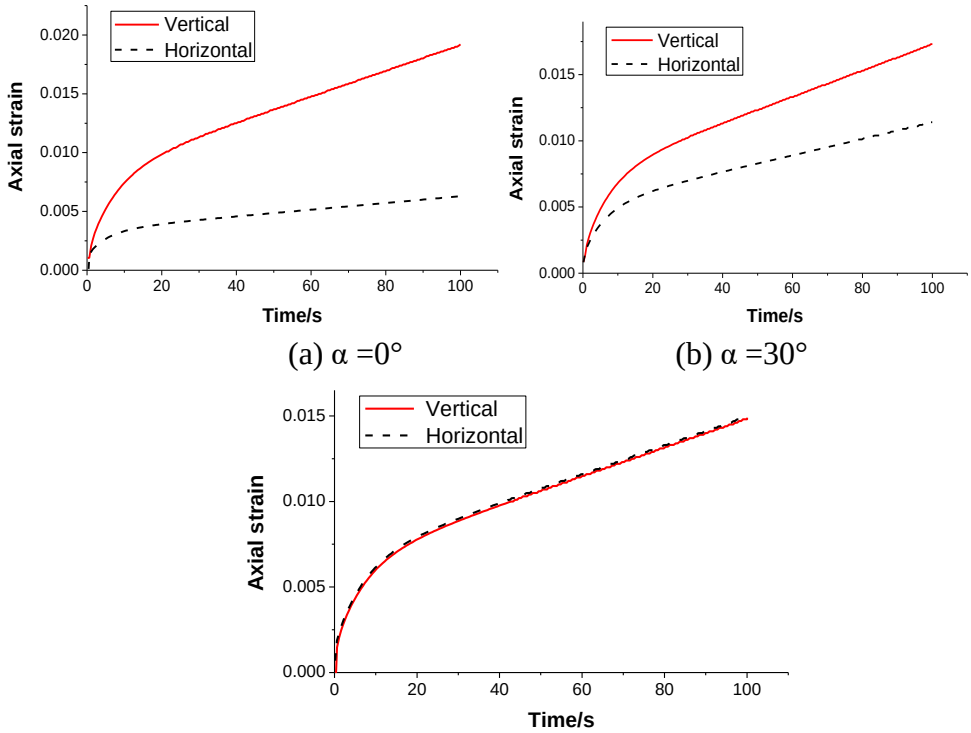

(a) α =0° (b) α =30°

(c) α =45°

Figure 7. Creep strain of DE models with different aggregate orientations.

EFFECT OF AGGREGATE SPHERICITY

When the aggregate orientations are 0°, 30° and 45°, the sphericity was varied

to be 0.7, 0.8, 0.9 and 1.0. Ten digital AC specimens with different aggregate orientations and sphericity were developed. The aggregates with different sphericity were shown in FIG. 8. Simulation of uniaxial creep tests were performed on the ten cubic digital AC specimens in horizontal and vertical directions. A static load of 0.7 MPa was applied. ε_{max} and ε_{min} were assumed to be the maximum and minimum creep strain in both directions. $\varepsilon_{min}/\varepsilon_{max}$ was adopted to represent the difference between the creep strain in both directions, and the smaller $\varepsilon_{min}/\varepsilon_{max}$ is, the more obvious the creep anisotropy is. The results were shown in FIG. 9.

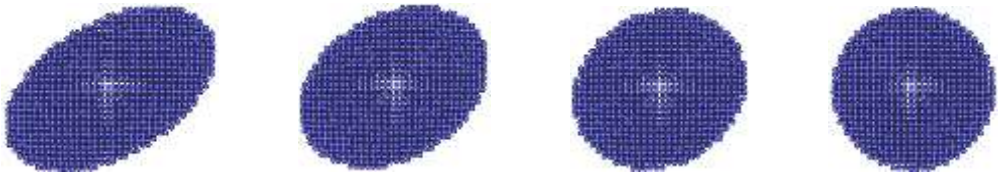

(a) SP=0.7 **(b) SP=0.8** **(c) SP=0.9** **(d) SP=1.0**

Figure 8. Ellipsoid aggregates with different sphericities.

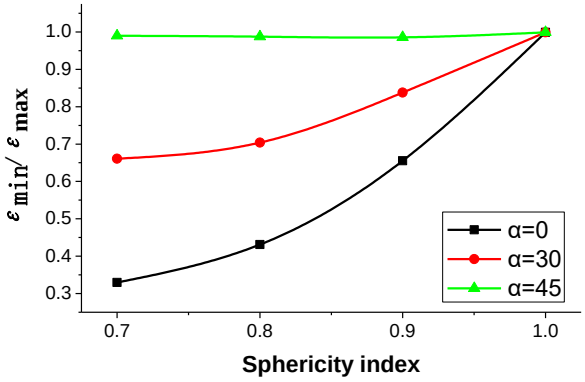

Figure 9. $\varepsilon_{min}/\varepsilon_{max}$ of DE models with different aggregate sphericity.

It can be seen from FIG. 9, when the aggregate orientation is 0°, the difference between the creep strain in horizontal and vertical directions decreased fast with increasing aggregate sphericity. When the aggregate orientation is 30°, the difference between the creep strain in both directions decreased more slowly. When the aggregate orientation is 45°, the difference between the creep strain in both directions is not obvious. The reason is that the difference between the creep strain in the horizontal and vertical directions is indeed slight when the aggregate orientation is 45°, as can be seen from FIG. 7 (c). It was observed that the difference between the creep strain in both directions decreased with increasing aggregate sphericity which indicated more slight creep anisotropy, especially when projected length of aggregates varied greatly in different directions.

CONCLUSIONS

This paper developed a 3D micromechanical model using discrete element method to investigate the effect of internal structure on creep anisotropy of AC. In the developed DE model, the accurate volumetric properties of aggregates,

asphalt mastic, and air voids could be represented. The aggregate morphology could also be desirably controlled. Simulation of uniaxial creep tests were conducted on a number of cubic digital AC specimens with different aggregate orientations and sphericity. The following conclusions were observed:

1) The longer projected length of aggregates in loading direction, the smaller the creep strain is. The creep strain of AC was much smaller in the major axis direction of aggregate orientation as compared with the minor one.
2) The creep anisotropy of AC became obvious with decreasing aggregate sphericity, especially when projected length of aggregates varied greatly in different directions.

ACKNOWLEDGMENTS

The study is financially supported by the Natural Science Foundation of Jiangsu Province (BK20140109) and the Research Foundation of Nanjing Institute of Technology (YKJ201512 and YKJ201428).

REFERENCES

[1] Masad E, Tashman L, Somedavan N, et al. Micromechanics-based analysis of stiffness anisotropy in asphalt mixtures. *Journal of Materials in Civil Engineering*, 2002; 14(5):374-383.

[2] Wang L, Hoyos L R, Wang J, et al. Anisotropic properties of asphalt concrete: characterization and implications for pavement design and analysis. *Journal of Materials in Civil Engineering*, 2005; 17(5):535-543.

[3] Mamlouk M S, Witczak M W, Kaloush K E, et al. Effect of anisotropy on compressive and tensile properties of asphalt mixtures. *Journal of Testing and Evaluation*, 2002; 30(5):432-438.

[4] Tutumluer E, Little D N, Kim S H. Validated model for predicting field performance of aggregate base courses. *Transportation Research Record*, 2003 (1837):41-49.

[5] Tutumluer, E. and Thompson, M R. Anisotropic modeling of granular bases inflexible pavements. *Transportation Research Record*, 1997(1577): 18-26.

[6] Liang R Y, Alfoul B A, Khasawneh M. Laboratory investigation of anisotropic behaviour of HMA. International conference on perpetual pavement, Columbus, Ohio, 2006.

[7] Zhang Y, Luo R, Lytton R L. Microstructure-Based Inherent Anisotropy of Asphalt Mixtures. *Journal of Materials in Civil Engineering*, 2011, 23(10): 1473-1482.

[8] Stakston, A D, Bahia, H U, and Bushek, J J. Effect of fine aggregate angularity on compaction and shearing resistance of asphalt mixtures. *Transportation Research Record* 2002 (1789): 14-24.

[9] Pan, T, Tutumluer, E, and Carpenter, S H. Effect of coarse aggregate morphology on permanent deformation behavior of hot mix asphalt. *Journal of Transportation Engineering*, 2006, 132(7): 580-589.

[10] Liu, Y, and You, Z. Visualization and simulation of asphalt concrete with randomly generated three-dimensional models. *Journal of Computing in Civil Engineering*, 2009, 23(6), 340-347.

[11] Masad E, Jandhyala V K, Dasgupta N, et al. Characterization of air void distribution in asphalt mixes using X-ray computed tomography. *Journal of Materials in Civil Engineering*, 2002; 14(2):122-129.
[12] Masad E, Muhunthan B, Shashidhar N, et al. Internal structure characterization of asphalt concrete using image analysis. *Journal of Computing in Civil Engineering*, 1999; 13(2): 88-95.
[13] Liu Y, Dai Q, You, Z. Viscoelastic model for discrete element simulation of asphalt mixtures [J]. *Journal of Engineering Mechanics*, 2009, 135(4): 324-333.
[14] Thornton C. The conditions for failure of a face-centered cubic array of uniform rigid spheres [J]. *Geotechnique*, 1979, 29(4): 441-459.
[15] Buttlar W G, You Z. Discrete element modeling of asphalt concrete: microfabric approach. *Transportation Research Record*, 2001(1757): 111-118.
[16] You Z, Buttlar W G. Discrete element modeling to predict the modulus of asphalt concrete mixtures. *Journal of Materials in Civil Engineerin*g, 2004, 16(2): 140-146.
[17] Huang X, Fan Y, Zhao Y, et al. Investigation and test of expressway asphalt pavement high-temperature performance. *Journal of Highway and Transportation Research and Development*, 2007, 24(5): 16-20.
[18] Masad, E., Al-Rousan, T., Button, J., et al. Test methods for characterizing aggregate shape, texture, and angularity. NCHRP Report 555, Transportation Research Board, Washington, DC, 2007.